MATERIALS CHEMISTRY
FRONTIERS

RESEARCH ARTICLE

View Article Online
View Journal | View Issue

Cite this: *Mater. Chem. Front.*, 2018, **2**, 700

A carbon–oxygen-bridged hexacyclic ladder-type building block for low-bandgap nonfullerene acceptors†

Ting Li,‡[ab] Honghong Zhang,‡[b] Zuo Xiao,[b] Jeromy J. Rech,[c] Helin Niu,*[a] Wei You*[c] and Liming Ding*[b]

Received 5th January 2018,
Accepted 24th January 2018

DOI: 10.1039/c8qm00004b

rsc.li/frontiers-materials

A hexacyclic carbon–oxygen-bridged ladder-type unit, CO_i6, was developed. Three nonfullerene acceptors (CO_i6IC, CO_i6FIC and CO_i6DFIC) based on CO_i6 were prepared. They present low optical bandgaps of 1.31–1.37 eV and strong absorbance in the near-infrared region. A 9.12% power conversion efficiency was achieved from the solar cells based on CO_i6FIC and a wide-bandgap copolymer donor (FTAZ).

Recently, acceptor–donor–acceptor (A–D–A) small molecules have emerged as efficient acceptor materials for organic solar cells (OSCs).[1] These molecules generally consist of a ladder-type electron-donating core unit and two strong electron-withdrawing end units.[2] The merits of A–D–A acceptors are as follows: (1) tunable energy levels and good electron mobility to match donor materials; (2) strong visible and near-infrared (NIR) absorption to generate more excitons; (3) out-of-plane side chains to avoid over aggregation and to realize optimal morphology.[3] Over 14% power conversion efficiency (PCE) was first reported by Ding *et al.*[4]

Molecular engineering *via* tailoring the structures of core units, end units and the side chains is the key toward high-performance A–D–A nonfullerene acceptors.[5] Recently, our group has developed novel carbon–oxygen-bridged (CO-bridged) ladder-type core units for making efficient A–D–A acceptors.[6] Compared with carbon-bridged (C-bridged) units, CO-bridged units show enhanced electron-donating capability and planarity. CO-Bridged A–D–A acceptors present narrower bandgaps, stronger light-harvesting capability, higher electron mobility and better photovoltaic performance.[6] Low-bandgap nonfullerene materials have attracted great attention due to their potential application in semi-transparent solar cells,[7] tandem solar cells,[8] and photodetectors.[9] Therefore, developing new low-bandgap CO-bridged A–D–A acceptors is quite necessary. Here, we report the preparation of a hexacyclic CO-bridged ladder-type building block, CO_i6, and the use of CO_i6 in making three low-bandgap A–D–A acceptors, CO_i6IC, CO_i6FIC and CO_i6DFIC (Fig. 1). The optical, electrochemical properties and the photovoltaic performance of CO_i6-based acceptors were investigated. Fluorine-substitution in the end units significantly affects the performance of the acceptors. Solar cells based on CO_i6FIC and a wide-bandgap copolymer donor, poly(4-(5-(4,8-bis(3-butylnonyl)benzo[1,2-*b*:4,5-*b*′]dithiophen-2-yl)thiophen-2-yl)-2-(2-butyloctyl)-5,6-difluoro-7-(thiophen-2-yl)-2*H*-benzo[*d*][1,2,3]triazole) (FTAZ),[10] gave a PCE of 9.12%.

The synthetic route is shown in Scheme 1. Stille coupling of (3,6-dimethoxythieno[3,2-*b*]thiophene-2,5-diyl)bis(trimethylstannane) and 2-ethylhexyl 2-bromothiophene-3-carboxylate gave compound **1** in 83% yield. Treating compound **1** with BBr_3 afforded the demethylated compound **2** in 95% yield. Compound **2** was quantitatively converted to bislactone **3** *via* an acid-promoted intramolecular transesterification.[6b] The addition of four equivalents of Grignard reagent to **3** followed by an intramolecular dehydration cyclization afforded CO_i6 in 86% yield.[11] "i" indicates that C–O bonds point to the core of the molecule (inward), and "6" stands for six fused rings. Deprotonation of CO_i6 by BuLi followed by adding *N*,*N*-dimethylformamide (DMF) produced CO_i6–CHO in 80% yield. Finally, Knoevenagel condensation of CO_i6–CHO with 1,1-dicyanomethylene-3-indanone (IC), monofluoro-substituted IC (FIC) or difluoro-substituted IC (DFIC) afforded CO_i6IC, CO_i6FIC and CO_i6DFIC in 90%, 94% and 86% yields, respectively. The structures of the compounds were confirmed by nuclear magnetic resonance (NMR) and mass spectroscopy (see ESI†). These compounds show good solubility in common solvents such as chloroform, toluene and chlorobenzene.

[a] *School of Chemistry & Chemical Engineering, Anhui Province Key Laboratory of Chemistry for Inorganic/Organic Hybrid Functionalized Materials, Anhui University, Hefei 230601, China. E-mail: niuhelin@ahu.edu.cn*
[b] *Center for Excellence in Nanoscience (CAS), Key Laboratory of Nanosystem and Hierarchical Fabrication (CAS), National Center for Nanoscience and Technology, Beijing 100190, China. E-mail: ding@nanoctr.cn*
[c] *Department of Chemistry, University of North Carolina at Chapel Hill, NC 27599, USA. E-mail: wyou@unc.edu*

† Electronic supplementary information (ESI) available: Materials preparation and characterization, solar cells fabrication and measurements. See DOI: 10.1039/c8qm00004b

‡ T. Li and H. Zhang contributed equally to this work.

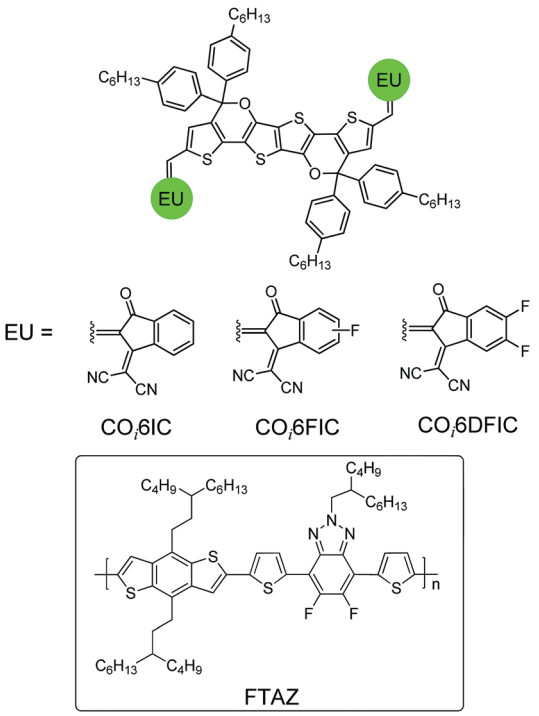

Fig. 1 The structures of CO$_i$6IC, CO$_i$6FIC, CO$_i$6DFIC and FTAZ.

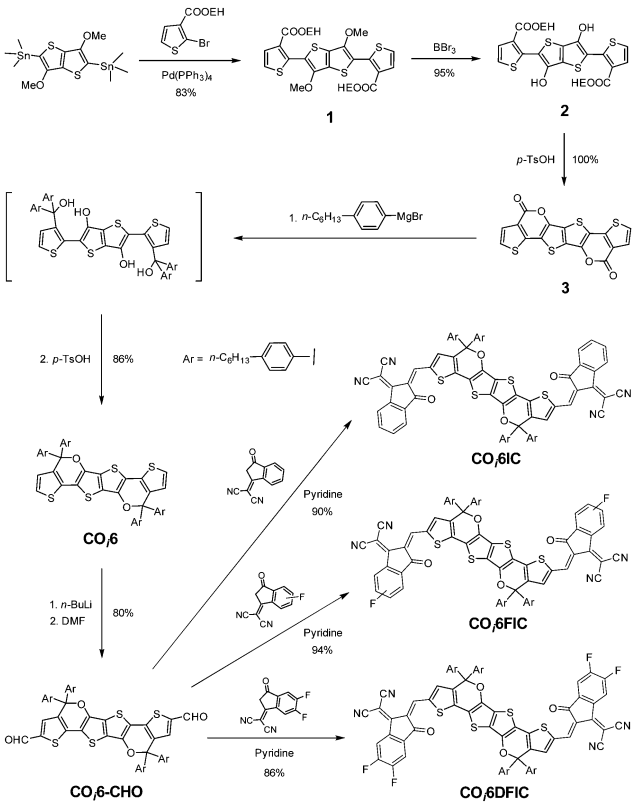

Scheme 1 The synthetic routes for CO$_i$6IC, CO$_i$6FIC and CO$_i$6DFIC.

The absorption spectra for CO$_i$6IC, CO$_i$6FIC, CO$_i$6DFIC and FTAZ in chloroform and as films are shown in Fig. S15 (ESI†) and Fig. 2, respectively. In solution, CO$_i$6IC, CO$_i$6FIC and

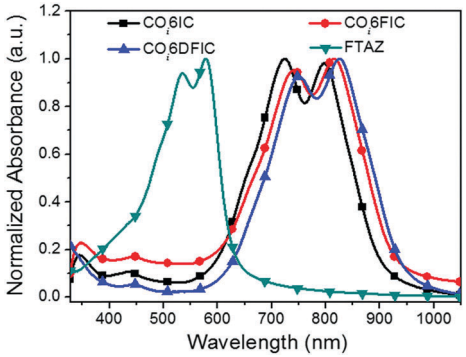

Fig. 2 Absorption spectra for CO$_i$6IC, CO$_i$6FIC, CO$_i$6DFIC and FTAZ films.

CO$_i$6DFIC show a strong intramolecular charge transfer (ICT) band at 600–850 nm, with a low-energy peak at 755 nm, 764 nm and 769 nm, respectively, and a shoulder absorption at 697 nm, 701 nm and 702 nm, respectively (Table 1). For films, the absorption show bathochromic shifts and the shoulder absorption intensifies. From solution to film, the redshifts for the low-energy peaks of CO$_i$6IC, CO$_i$6FIC and CO$_i$6DFIC are 40 nm, 51 nm and 55 nm, respectively, suggesting that the fluorination on IC unit enhanced the intermolecular interaction. The optical bandgaps (E_g^{opt}) estimated from the absorption onsets of CO$_i$6IC, CO$_i$6FIC and CO$_i$6DFIC films are 1.37 eV, 1.34 eV and 1.31 eV, respectively. Small E_g^{opt} suggests strong electron-donating capability of CO$_i$6 unit.[12] Fluorine atoms enhance electron-withdrawing capability of the end units and strengthen the ICT, leading to a bandgap shrink. FTAZ film absorbs 350–650 nm light, which is complementary to CO$_i$6 acceptors (600–950 nm). The energy levels estimated from CV measurements are shown in Fig. 3.[13] The highest occupied molecular orbital (HOMO) levels for CO$_i$6IC, CO$_i$6FIC and CO$_i$6DFIC are −5.57 eV, −5.60 eV and −5.64 eV, respectively, and the lowest unoccupied molecular orbital (LUMO) levels are −3.86 eV, −3.93 eV and −4.04 eV, respectively. Fluorine atoms lower both HOMO and LUMO levels, but they lower LUMO more. The donor FTAZ exhibits a HOMO at −5.36 eV and a LUMO at −3.05 eV.

Bulk heterojunction solar cells with a structure of ITO/ZnO/FTAZ:acceptor/MoO_3/Ag were fabricated to evaluate the performance of CO$_i$6 acceptors.[14] The optimized conditions for FTAZ:CO$_i$6IC, FTAZ:CO$_i$6FIC and FTAZ:CO$_i$6DFIC solar cells are the same: a D/A ratio of 1 : 1.6 (w/w), an active layer thickness of ~85 nm and 0.2 vol% 1,8-diiodooctane (DIO) as the additive (Tables S1–S9, ESI†). *J*–*V* curves and external quantum efficiency (EQE) spectra for the best cells are shown in Fig. 4, and the performance data are listed in Table 2. Fluorine substitution can significantly affect the performance of CO$_i$6 acceptors. The open-circuit voltages (V_{oc}) for CO$_i$6IC, CO$_i$6FIC and CO$_i$6DFIC cells are 0.82 V, 0.75 V and 0.67 V, respectively. V_{oc} decreasing along with fluorine substitution is due to LUMO descending, since V_{oc} is proportional to ($LUMO_{acceptor}$–$HOMO_{donor}$).[15] In contrast, the short-circuit current densities (J_{sc}) increase along with fluorine substitution. J_{sc} of 17.45 mA cm^{-2}, 19.38 mA cm^{-2} and 20.98 mA cm^{-2} were obtained from CO$_i$6IC, CO$_i$6FIC and CO$_i$6DFIC cells, respectively. With fluorine substitution,

Table 1 Optical and electrochemical data for the acceptors

Acceptors	λ_{sol} [nm]	λ_{film} [nm]	λ_{on} [nm]	$E_g^{opt\,a}$ [eV]	E_{ox}^{on} [V]	E_{red}^{on} [V]	HOMO^b [eV]	LUMO^c [eV]	$E_g^{ec\,d}$ [eV]
CO_i6IC	697, 755	722, 795	903	1.37	0.77	−0.94	−5.57	−3.86	1.71
CO_i6FIC	701, 764	739, 815	927	1.34	0.80	−0.87	−5.60	−3.93	1.67
CO_i6DFIC	702, 769	749, 824	945	1.31	0.84	−0.76	−5.64	−4.04	1.60

^{a} $E_g^{opt} = 1240/\lambda_{on}$. ^{b} HOMO = $-(E_{ox}^{on} + 4.8)$. ^{c} LUMO = $-(E_{red}^{on} + 4.8)$. ^{d} E_g^{ec} = LUMO − HOMO.

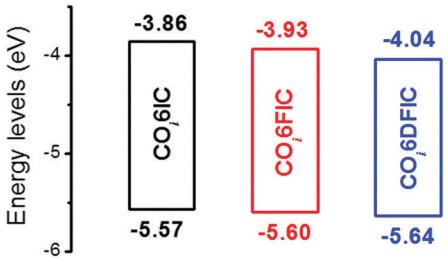

Fig. 3 Energy level diagram.

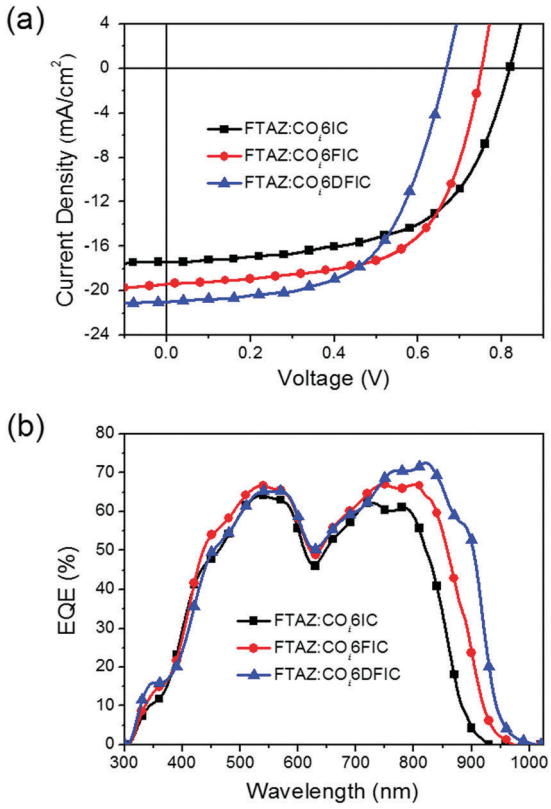

Fig. 4 *J*–*V* curves (a) and EQE spectra (b) for the solar cells.

the EQE spectra broaden and intensify (Fig. 4b). The broadening of EQE spectra results from the enhanced light-harvesting capability of the acceptors, while enhanced EQE might result from the improved charge generation and transport in the active layer. The integrated photocurrent densities from EQE spectra are consistent with J_{sc} from *J*–*V* measurements (Table 2). The fill factors (FF) for CO_i6IC, CO_i6FIC and CO_i6DFIC cells are 59.0%, 62.6% and 58.9%, respectively. CO_i6FIC solar cells gave the highest PCE of 9.12%.

Table 2 Performance data for the solar cells

D:A	V_{oc} [V]	J_{sc} [mA cm^{-2}]	FF [%]	PCE [%]
FTAZ:CO_i6IC	0.82	17.45 (16.93)^a	59.0	8.43 (8.35)^b
FTAZ:CO_i6FIC	0.75	19.38 (19.27)	62.6	9.12 (9.02)
FTAZ:CO_i6DFIC	0.67	20.98 (20.39)	58.9	8.25 (8.11)

^{a} The data in the parentheses are integrated current density from EQE spectra. ^{b} The data in the parentheses are averages for 10 cells.

To understand the fluorination effect on the photovoltaic performance of CO_i6 acceptors, we first studied the exciton dissociation probabilities (P_{diss}) in different cells (Fig. 5a).[16] P_{diss} for CO_i6IC, CO_i6FIC and CO_i6DFIC cells are 90.4%, 94.1% and 93.9%, respectively. Higher P_{diss} for CO_i6FIC and CO_i6DFIC cells indicate that fluorination favors the generation of free charge carriers. This explains the higher EQE and J_{sc} of CO_i6FIC and CO_i6DFIC cells than that of CO_i6IC cells. We studied bimolecular recombination by plotting J_{sc} against light intensity (P_{light}) (Fig. 5b).[17] The data were fitted to a power law: $J_{sc} \propto P_{light}^{\alpha}$. The α values for CO_i6IC, CO_i6FIC and CO_i6DFIC cells are 0.978, 0.987 and 0.983,

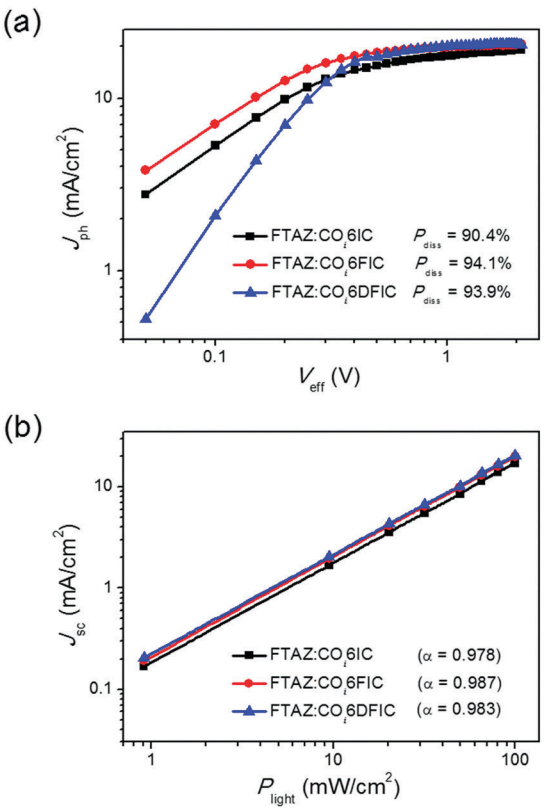

Fig. 5 (a) J_{ph}–V_{eff} plots; (b) J_{sc}–P_{light} plots.

respectively, suggesting that solar cells using fluorinated acceptors have less charge recombination. Charge carrier mobilities were evaluated by using space charge limited current (SCLC) method (Fig. S17 and S18, ESI†).[18] Compared with FTAZ:CO_i6IC blend film, the hole and electron mobilities (μ_h and μ_e) simultaneously got improved in FTAZ:CO_i6FIC and FTAZ:CO_i6DFIC blend films (Table S10, ESI†). FTAZ:CO_i6FIC film shows the highest μ_h and μ_e of 1.45×10^{-4} cm^2 V^{-1} s^{-1} and 2.07×10^{-5} cm^2 V^{-1} s^{-1}, respectively. FTAZ:CO_i6FIC film presents the most balanced charge carrier transport, thus delivering the highest FF.

Film morphology was studied by using atomic force microscope (AFM) (Fig. S19, ESI†). FTAZ:CO_i6FIC blend film gives the smoothest surface among the three films. The root-mean-square roughnesses for FTAZ:CO_i6IC, FTAZ:CO_i6FIC and FTAZ:CO_i6DFIC films are 2.33 nm, 0.94 nm and 1.87 nm, respectively. FTAZ:CO_i6FIC blend film presents the finest nanofibers with diameters around 12 nm. With appropriate fluorination at the end units of the acceptor, the donor and acceptor materials can present a suitable miscibility and can make ideal nanoscale phase separation for efficient charge generation and transport, thus delivering optimal photovoltaic performance.

Conclusions

In summary, a CO-bridged hexacyclic core unit (CO_i6) and three A–D–A nonfullerene acceptors were developed. Owing to the strong electron-donating capability of CO_i6, these acceptors present narrow optical bandgaps and good NIR absorption. The energy levels, light absorption, mobilities, and the miscibility between donor and acceptor materials can be tuned *via* fluorination. Solar cells based on a wide-bandgap polymer donor (FTAZ) and CO_i6 acceptors gave decent PCEs, and FTAZ:CO_i6FIC cells delivered the highest PCE of 9.12%. This work also demonstrates the great potential of CO-bridged low-bandgap nonfullerene acceptors.

Conflicts of interest

There are no conflicts to declare.

Acknowledgements

We greatly appreciate National Natural Science Foundation of China (U1401244, 21374025, 21372053, 21572041, 51503050, 51773045, 21772030 and 21704021), National Key Research and Development Program of China (2017YFA0206600) and the Youth Association for Promoting Innovation (CAS) for financial support. H. Niu thanks National Natural Science Foundation of China (51771001, 21471001 and 21575001) and Natural Science Foundation of Anhui Province (1508085MB3) for financial support.

References

1 (*a*) Y. Lin and X. Zhan, *Mater. Horiz.*, 2014, **1**, 470; (*b*) W. Chen and Q. Zhang, *J. Mater. Chem. C*, 2017, **5**, 1275; (*c*) S. Li, Z. Zhang, M. Shi, C.-Z. Li and H. Chen, *Phys. Chem. Chem. Phys.*, 2017, **19**, 3440.
2 Y. Lin, J. Wang, Z. G. Zhang, H. Bai, Y. Li, D. Zhu and X. Zhan, *Adv. Mater.*, 2015, **27**, 1170.
3 Y. Lin, F. Zhao, Y. Wu, K. Chen, Y. Xia, G. Li, S. K. K. Prasad, J. Zhu, L. Huo, H. Bin, Z. G. Zhang, X. Guo, M. Zhang, Y. Sun, F. Gao, Z. Wei, W. Ma, C. Wang, J. Hodgkiss, Z. Bo, O. Inganäs, Y. Li and X. Zhan, *Adv. Mater.*, 2017, **29**, 1604155.
4 Z. Xiao, X. Jia and L. Ding, *Sci. Bull.*, 2017, **62**, 1562.
5 (*a*) J. Wang, W. Wang, X. Wang, Y. Wu, Q. Zhang, C. Yan, W. Ma, W. You and X. Zhan, *Adv. Mater.*, 2017, **29**, 1702125; (*b*) S. Dai, F. Zhao, Q. Zhang, T.-K. Lau, T. Li, K. Liu, Q. Ling, C. Wang, X. Lu, W. You and X. Zhan, *J. Am. Chem. Soc.*, 2017, **139**, 1336; (*c*) Y. Lin, F. Zhao, Q. He, L. Huo, Y. Wu, T. C. Parker, W. Ma, Y. Sun, C. Wang, D. Zhu, A. J. Heeger, S. R. Marder and X. Zhan, *J. Am. Chem. Soc.*, 2016, **138**, 4955.
6 (*a*) Z. Xiao, F. Liu, X. Geng, J. Zhang, S. Wang, Y. Xie, Z. Li, H. Yang, Y. Yuan and L. Ding, *Sci. Bull.*, 2017, **62**, 1331; (*b*) Z. Xiao, X. Jia, D. Li, S. Wang, X. Geng, F. Liu, J. Chen, S. Yang, T. P. Russell and L. Ding, *Sci. Bull.*, 2017, **62**, 1494.
7 (*a*) W. Wang, C. Yan, T.-K. Lau, J. Wang, K. Liu, Y. Fan, X. Lu and X. Zhan, *Adv. Mater.*, 2017, **29**, 1701308; (*b*) F. Liu, Z. Zhou, C. Zhang, J. Zhang, Q. Hu, T. Vergote, F. Liu, T. P. Russell and X. Zhu, *Adv. Mater.*, 2017, **29**, 1606574.
8 W. Liu, S. Li, J. Huang, S. Yang, J. Chen, L. Zuo, M. Shi, X. Zhan, C.-Z. Li and H. Chen, *Adv. Mater.*, 2016, **28**, 9729.
9 W. Wang, F. Zhang, H. Bai, L. Li, M. Gao, M. Zhang and X. Zhan, *Nanoscale*, 2016, **8**, 5578.
10 S. C. Price, A. C. Stuart, L. Yang, H. Zhou and W. You, *J. Am. Chem. Soc.*, 2011, **133**, 4625.
11 L. Dou, C.-C. Chen, K. Yoshimura, K. Ohya, W.-H. Chang, J. Gao, Y. Liu, E. Richard and Y. Yang, *Macromolecules*, 2013, **46**, 3384.
12 H. Zhou, L. Yang and W. You, *Macromolecules*, 2012, **45**, 607.
13 Z. Xiao, G. Ye, Y. Liu, S. Chen, Q. Peng, Q. Zuo and L. Ding, *Angew. Chem., Int. Ed.*, 2012, **51**, 9038.
14 Z. Xiao, X. Geng, D. He, X. Jia and L. Ding, *Energy Environ. Sci.*, 2016, **9**, 2114.
15 B. P. Rand, D. P. Burk and S. R. Forrest, *Phys. Rev. B: Condens. Matter Mater. Phys.*, 2007, **75**, 115327.
16 J.-L. Wu, F.-C. Chen, Y.-S. Hsiao, F.-C. Chien, P. Chen, C.-H. Kuo, M. H. Huang and C.-S. Hsu, *ACS Nano*, 2011, **5**, 959.
17 M. An, F. Xie, X. Geng, J. Zhang, J. Jiang, Z. Lei, D. He, Z. Xiao and L. Ding, *Adv. Energy Mater.*, 2017, **7**, 1602509.
18 J. Cao, Q. Liao, X. Du, J. Chen, Z. Xiao, Q. Zuo and L. Ding, *Energy Environ. Sci.*, 2013, **6**, 3224.